Optimization of the Average-Dispersion Range for Long-Haul Dispersion-Managed Soliton Systems

T. I. Lakoba and G. P. Agrawal, *Fellow, IEEE*

***Abstract*—We consider limitations on unfiltered transmission of dispersion-managed solitons, arising from the Gordon–Haus jitter, adjacent pulse interaction, and signal-to-noise degradation. We maximize the range of allowed values of average dispersion, thereby providing the first step in optimization of dispersion maps for wavelength-division-multiplexed lightwave systems. As specific examples, we consider dispersion maps made of several different types of optical fiber and study their performance for transmission of 10–40 Gb/s channels over distances in the range from 3000 km to 10 000 km.**

***Index Terms*—Broad-band optical fiber communications, dispersion management, optical noise, optical solitons.**

I. Introduction

THE GOAL OF this study is to compare the performance of various types of dispersion maps for long-haul soliton data transmission. Our basic idea is to find the maximum allowed range of values for the average dispersion, so that the maximum number of wavelength-division multiplexed (WDM) channels can be transmitted at a given bit rate per channel. Here we take into account the fact that the average dispersion, D_{av}, as seen by different channels, is different due to the third-order dispersion.

Clearly, the scope of the problem we have outlined above is too broad, and too complex, to be satisfactorily treated within one study. Therefore, we had to make a number of simplifying assumptions. First and foremost, we considered only those impairments that occur for single-channel transmission. That is, no limitations due to pulse collisions or gain fluctuations in different wavelength channels, were considered. It is clear that maximizing the range of D_{av}, while accounting only for single-channel impairments is the necessary first step in the design of any WDM system. This study aims at providing the guidelines in taking that first step by examining what types of dispersion maps can potentially yield high transmission capacity.

Our second important assumption is that the dispersion-managed (DM) system under consideration has no in-line control elements, such as narrow-band filters or synchronous modulators. Both filters and modulators are known to be able to improve the quality of transmission; however, there also exist practical issues which make the use of these elements in a real long-haul system difficult.

Manuscript received September 27, 1999; revised May 31, 2000. This work was supported in part by the National Science Foundation under Grants PHY94-15583 and ECS-9903580.

The authors are with the Rochester Theory Center of Optical Science and Engineering, Institute of Optics, University of Rochester, Rochester, NY 14627 USA (e-mail: lakobati@optics.rochester.edu; gpa@optics.rochester.edu).

Publisher Item Identifier S 0733-8724(00)09816-9.

The lower limit for the average dispersion is known to be set by degradation of the signal-to-noise ratio (SNR) resulting from accumulation of spontaneous-emission noise from amplifiers [1]. The two principal impairments setting the upper bound for D_{av} are the Gordon–Haus (GH) timing jitter and the interaction of adjacent pulses. Strictly speaking, the latter two effects are to be considered simultaneously, as the GH jitter affects the pulse center separation, which is a critical parameter for soliton interaction [2], [29], [30]. However, at present, there is no theory that correctly describes the interaction of DM solitons even neglecting the GH jitter (at least in the range of parameters that is of interest for this study). Therefore we have to adopt the following procedure. First, we calculate the upper bound for D_{av} as given by the GH jitter alone [3], [31]. Then we numerically simulate the full nonlinear Schrödinger (NLS) equation, *without the noise source* and with the D_{av} determined at the previous stage, and find how much the pulse separation would decrease due to the interaction alone. Finally, we adjust the value of D_{av} in a certain way (cf. Section II).

It is well known that in a DM system with a given D_{av}, the GH jitter is suppressed, in comparison with the jitter in a uniform-dispersion fiber with the same dispersion D_{av} by a so-called energy enhancement factor (EEF) [4]. The latter is known to depend strongly on the location of the amplifier(s) inside the dispersion map [5]–[8]. Furthermore, the strength of pulse interactions and the EEF follow roughly the same dependence on details of the dispersion map [8], [9]. That is, a larger EEF results in more effective jitter suppression but also in stronger pulse interaction. Thus, the location of the amplifier(s) inside the map must be a critical parameter in any DM optimization. However, since we do not have a formula for determining the effect of pulse interaction and thus have to resort to full numerical simulations, it is very important to reduce the number of free parameters in the problem. Therefore, we vary the amplifier location only within the shorter (compensating) section of fiber and only for one of the map configurations (cf. Section III). It is likely that not (fully) optimizing the location of the amplifier could change our results by a factor of order two or so. However, such accuracy is adequate for the main goal of this study, which is to reveal *trends* that can lead to design optimization rather than to obtain quantitatively correct results.

We do not consider contributions to the timing jitter coming from the acoustic effect and the polarization mode dispersion (PMD) [10]. The reason for not considering the acoustic effect is that it only contributes a slow-time component to the jitter, which can be eliminated by a proper adjustment of the receiver [11], [32]. The jitter coming from the combined effect of the PMD and spontaneous-emission noise of amplifiers [12] can

be estimated to be much less than the GH jitter for the types of fiber considered here and for $(D_{av})_{\max} > 0.1$ ps/nm/km, which we always find to be the case in this study. Also, we do not include effects of third-order dispersion and stimulated Raman scattering on single channel transmission, since these effects have been shown [13], [14] to be small for the combinations of bit rates and distances considered here.

The remainder of this paper is organized as follows. In Section II, we present the theory from which the upper and lower bounds for D_{av} are found. Section III describes our optimization procedure. Section IV contains the main results of this study: it shows the estimates for the maximum number of WDM channels that various types of dispersion maps can transmit, assuming only the single-channel impairments. Main results are summarized in Section V.

II. Theory

A. Unperturbed DM Soliton

Our model is based on the standard NLS equation that governs propagation of optical pulses in fibers

$$i\frac{\partial A}{\partial Z} - \frac{1}{2}\beta_2(Z)\frac{\partial^2 A}{\partial T^2} + \gamma|A|^2 A = \frac{i}{2}\left[g(Z) - \alpha\right]A. \tag{1}$$

Here $\beta_2 = [-\lambda^2/(2\pi c)]D$, D is the dispersion coefficient, λ is the operating wavelength (assumed to be 1550 nm), c is the speed of light, and γ is the nonlinearity coefficient. The effect of fiber loss and its periodic compensation are included through the parameters α and $g(z)$, respectively. Changing their form, we can study various cases of lumped amplification, as well as the case of distributed amplification. In a DM system, $D(Z)$ is a piecewise-constant, periodic function with values D_1 and D_2 in the two sections of the dispersion map. The lengths of these two sections are L_1 and L_2, respectively, and $L_1 + L_2 = L_{\rm map}$, where $L_{\rm map}$ is the period of the map.

It is common to introduce normalized variables and write (1) in a nondimensional form. We introduce new variables as

$$z = Z/L_{\rm map}, \quad T = T/T_{\rm DM}$$
$$u = A\exp\left(\tfrac{1}{2}\alpha Z - \tfrac{1}{2}\int_0^Z g(Z')\,dZ'\right)\Big/\sqrt{P_0} \tag{2}$$

where $T_{\rm DM}$ is a time-scaling parameter chosen such that

$$T_{\rm DM} = \left([\lambda^2/(2\pi c)]|D_1 - D_2|L_1L_2/L_{\rm map}|\right)^{1/2}. \tag{3}$$

The parameter P_0 is a reference power used for normalization and equals the peak power in an idealized lossless fiber. Its relation to the average pulse power in a fiber with periodically compensated loss is specified after (11). In terms of the normalized variables z, τ, and u, we obtain the following nondimensional form of the NLS equation:

$$i\frac{\partial u}{\partial z} + \frac{1}{2}d(z)\frac{\partial^2 u}{\partial \tau^2} + \epsilon\left(\frac{1}{2}d_0\frac{\partial^2 u}{\partial \tau^2} + G(z)|u|^2 u\right) = 0 \tag{4}$$

where the periodic coefficient $G(z) = \exp(L_{\rm map}(\int_0^z g(z')\,dz' - \alpha z))$ accounts for weakening of the nonlinear effects due to the fiber loss, and the nondimensional parameter ϵ is given by

$$\epsilon = \gamma P_0 L_{\rm map}. \tag{5}$$

This parameter measures the size of the nonlinearity compared to that of the local dispersion. In (4), the nondimensional dispersion coefficient is explicitly written as a sum of the constant average part

$$\epsilon d_0 = \frac{(D_1L_1 + D_2L_2)L_{\rm map}}{|D_1 - D_2|L_1L_2} \equiv \frac{D_{av}L_{\rm map}}{T_{\rm DM}^2}\left(\frac{\lambda^2}{2\pi c}\right) \tag{6}$$

and the periodic part

$$d(z) = \begin{cases} \mathrm{sgn}(D_1)L_{\rm map}/L_1, & 0 < z < L_1/L_{\rm map} \\ -\mathrm{sgn}(D_1)L_{\rm map}/L_2, & L_1/L_{\rm map} < z < 1 \end{cases} \tag{7}$$

whose average vanishes: $\int_0^1 d(z)\,dz = 0$.

In the regime of strong DM, local dispersion is much greater than both the average dispersion and nonlinearity; hence $\epsilon \ll 1$ in (4). The high local dispersion determines the functional form of the DM soliton in terms of chirped Hermite–Gaussian functions [15], [33], of which the largest is a chirped Gaussian

$$u_0 = \frac{\alpha_0}{\sqrt{1+i\delta}}\exp\left[-\frac{\tau^2}{2\tau_0^2(1+i\delta)} + i\phi(z)\right] \tag{8}$$

where

$$\delta \equiv \delta(z) = \delta_0 + \frac{1}{\tau_0^2}\int_0^z D(z')\,dz' \tag{9}$$

and the form of the phase $\phi(z)$ is not relevant to this study. The parameter δ is proportional to the chirp. The pulse width reaches its minimum, τ_0, at the points in the map where $\delta(z) = 0$. In Ref. [16] it was shown that higher-order Hermite–Gaussian functions may contribute to the evolution of a perturbed DM soliton by no more than 5–6% (this does not pertain to the interaction of adjacent DM solitons). Thus in what follows we do not consider those higher order terms.

With the Gaussian approximation for the pulse shape, and for a sufficiently small ϵ, the balance between the average dispersion and nonlinearity sets the following two conditions for the stationary propagation of a DM soliton

$$\mathrm{Im}I_2 = \epsilon\frac{C_I}{4\sqrt{2}}, \quad d_0 = |a_0|^2\tau_0^2\left(\frac{\mathrm{Re}I_2}{\sqrt{2}} + \epsilon\frac{C_R}{8}\right) \tag{10}$$

where the coefficient I_2 is obtained from

$$I_n = \int_0^1 \tilde{I}_n\,dz, \quad \tilde{I}_n = \frac{G(z)}{\sqrt{1+\delta}}\left(\frac{1+i\delta}{1-i\delta}\right)^{n/2}$$
$$n = 0, 1, 2, \ldots \tag{11}$$

The first condition in (10) determines the pulse initial chirp, and the second condition determines the relation among the pulse amplitude, width, and the average dispersion parameter d_0. These equations generalize those derived in [6], [17], [15], and [33] via including the next-order terms in ϵ. The factor $1/\mathrm{Re}I_2$ is proportional to the energy enhancement factor mentioned in Section I. The form of C_I and C_R is specified in the Appendix. The details of the periodic amplification

are included via the function $G(z)$ in the integrals I_n. This provides a uniform framework for dealing with both lumped and distributed amplification cases. Furthermore, the soliton amplitude, a_0, can always be normalized to unity by a proper choice of the reference power P_0, and we use this normalization in what follows. In such a case, the average DM soliton power equals $P_0 I_0$, where I_0 is defined by (11). Alternatively, the DM soliton energy immediately after an amplifier equals $\sqrt{\pi} G(z_{\rm amp}) P_0 T_{\rm DM} \tau_0$, where $G(z_{\rm amp})$ is the value of $G(z)$ at the amplifier's location.

When the nonlinearity and the average dispersion are small (i.e., $\epsilon \ll 1$), (9)–(11) indicate that the single parameter that determines properties of an unperturbed DM soliton is the normalized pulse width $\tau_0 = T_0/T_{\rm DM}$. Here T_0 is the minimum width of the Gaussian pulse, related to the full width at half maximum (FWHM) as $T_{\rm FWHM} = 2\sqrt{\ln 2} T_0$. For easy comparison with previous work, we use a related nondimensional parameter S, called the map strength and defined as follows:

$$S = \frac{1}{2\ln 2 \tau_0^2} = \frac{|(D_1 - D_{av})L_1 - (D_2 - D_{av})L_2|}{T_{\rm FWHM}^2} \left(\frac{\lambda^2}{2\pi c}\right) \quad (12)$$

where $D_{av} = (D_1 L_1 + D_2 L_2)/L_{\rm map}$. To support stationary propagation of a DM soliton at zero average dispersion, one requires a specific value $S = S_0$ where the quantity ${\rm Re} I_2$ vanishes [cf. the second of (10)]. Accordingly, the average dispersion should be "normal" for $S > S_0$. For both lossless and periodically amplified cases, the value of S_0 was found [6] to be approximately equal 4.7. When one takes into account the $O(\epsilon)$ terms in (10) (which should be done when the pulse power is sufficiently high), one finds that for $S > S_0$, the DM soliton can exist for either sign of average dispersion [18], [34], [35].

B. Upper and Lower Bounds for D_{av}

Since the soliton power is approximately proportional to the average dispersion [cf. (5) and (6)], the lower bound for D_{av} is imposed by the requirement that the SNR after. $N(= Z/L_{\rm amp} \gg 1)$ amplifiers be greater than a threshold necessary to maintain a given bit error rate (BER). Here Z is the *dimensional* total propagation distance. From [19], we find that

$${\rm SNR} = \frac{P_0 \tau_0 T_{\rm DM} \sqrt{\pi}}{(Z/L_{\rm amp}) n_{sp} h\nu (2M)(G-1)} \quad (13)$$

where

- n_{sp} spontaneous emission factor (we assume $n_{sp} = 1.5$);
- $h\nu$ energy of one photon;
- G total gain within one amplification stage.

The parameter M is identified with the number of independent degrees of freedom in one polarization of the signal (cf. [20], [21]). The factor two in front of M is included because the receiver is assumed to be sensitive to both polarizations. Equation (13) is written for the case of lumped amplification. For distributed amplification, the factor $(G-1)/L_{\rm amp}$ is replaced with α_{av}, the average loss coefficient. The relation between the SNR and the BER is established via the parameter Q, using the Gaussian approximation for the probability density of the detected signal [21]

$$Q = \sqrt{M} \frac{\rm SNR}{\sqrt{2{\rm SNR}+1}+1} \quad (14)$$

$${\rm BER} \approx \frac{\exp(-Q^2/2)}{\sqrt{2\pi} Q}. \quad (15)$$

The values 10^{-12} and 10^{-6} of BER, which we use later in this study, correspond to $Q \approx 7$ and $Q \approx 4.75$, respectively. Assuming $M = 8$, (14) yields SNR $\approx$ 17.2 and SNR $\approx$ 9.0, respectively. Using (5), (6), (13), and the main-order terms in (10), one obtains the following inequality for the average dispersion D_{av}:

$$D_{av} \geq {\rm SNR}(2M) n_{sp} h\nu (G-1)(Z/L_{\rm amp}) \frac{\tau_0 {\rm Re} I_2 T_{\rm DM}}{\sqrt{2\pi}} \left(\frac{2\pi c}{\lambda^2}\right). \quad (16)$$

In the case of distributed amplification, this equation is modified using $G - 1 = \alpha_{av} L_{\rm map}$. The nonlinearity coefficient γ corresponds to either section of the dispersion map; the specific choice affects I_2 via $G(z)$, so that the product in the numerator of (16) is not affected. Since this lower bound for D_{av} was found to yield rather small values of D_{av}, the $O(\epsilon)$ terms in (10) could be safely neglected.

The most restrictive upper bound for D_{av}, is set by the GH timing jitter and pulse interaction. The variance of the GH jitter is [3], [31]

$$\sigma_{\rm GH}^2 = \frac{n_{sp} h\nu (G-1)(L_{\rm map}/L_{\rm amp})}{\tau_0^3 T_{\rm DM} P_0 \sqrt{\pi}} \times F_{\rm GH}(z) \quad (17)$$

$$F_{\rm GH}(z) = 2\int_0^z (d(z') + \epsilon d_0)\, dz' \int_0^{z'} (d(z'') + \epsilon d_0)\,[z''+1]\, dz'' + 2\tau_0^2 \delta_{\rm amp} \int_0^z (d(z') + \epsilon d_0)\,[z'+1]\, dz' + z(\tau_0^4 + \tau_0^4 \delta_{\rm amp}^2) \quad (18)$$

where

- $z = Z/L_{\rm map}$ normalized distance;
- $[z]$ integer part of z;
- $\delta_{\rm amp}$ value of $\delta(z)$ evaluated at the amplifier.

Equation (17) is written for the case of one amplifier per map period; generalization to other cases is straightforward [3], [31]. The same equation can also be derived using the variational method [22] with a Gaussian ansatz.

The leading-order term on the right-hand side of (18) equals $(\epsilon d_0)^2 z^3/3$, i.e., its value for the conventional soliton in a uniform-dispersion fiber. In all cases considered, we found that the upper bound for D_{av} corresponds to $\epsilon d_0 = O(0.1)$. With $z = O(100)$, corresponding to a trans-oceanic distance, the size of the $O(z^2)$ term is estimated to be on the order of 10% of the leading term, and the $O(z)$ term is even smaller. Thus, when writing down the analytical expression for the upper bound (see (19), shown at the bottom of the next page), we retain only the $O(z^3)$ term in order to make that expression more transparent. However, in the numerical calculations, whose results are presented in Section IV, we use the full expression (18) for the variance of the GH jitter.

Further, we assume, as done in most studies, that the probability density $p(\delta\tau)$ of the deviation of the pulse from the center of the bit slot, is Gaussian with the variance $\sigma_{\rm GH}$. Then the probability of the pulse center to be found outside of the bit slot T_B equals $2\int_{T_B/2}^{\infty} p(\delta\tau)d(\delta\tau)$. For $T_B > 6\sigma_{\rm GH}$. this probability is approximated quite well by twice the right-hand side of (15), where Q is replaced with $Q_{\rm GH} \equiv T_B/(2\sigma_{\rm GH})$. Combining (17) and (18) with (5) and (10), we arrive at the following upper bound for the average dispersion, imposed by the GH jitter alone, as shown in (19), where $B = 1/T_B$ is the bit rate. Since ϵ, appearing in the denominator, is proportional to D_{av}, (19) provides an *implicit* upper bound for D_{av}. Our numerical code implements an iterative procedure to solve for the value of that upper bound, while taking into account all terms in (10) and (18).

To account for pulse interaction, we use the following simple trick. We numerically solve (4) with the parameter ϵd_0 found from (6) and (19). For a given propagation distance z we find the change, $\delta\tau_{int}$, in the pulse separation, that is due only to the interaction. We set the condition $\delta\tau_{int} > 0.4T_B$ to indicate pulse collision, when the interaction prohibits system operation that otherwise would have been allowed by the GH jitter alone. For smaller relative values of $\delta\tau_{int}$, we simply use inequality (19), but with an adjusted bit slot, $\tilde{T}_B = T_B - \delta\tau_{int}$. Thus, as the upper bound for D_{av} imposed by both the GH jitter and pulse interaction, we use an estimate

$$\tilde{D}_{av} = D_{av}(1 - \delta\tau_{int}B)^2. \tag{20}$$

In the absence of a theory that would have simultaneously accounted for both the GH jitter and pulse interactions, we have to resort to such a crude estimate to avoid time-prohibiting numerical simulations.

The last restriction that sets an independent upper bound for D_{av} is the following. It follows from (6) and (10) that D_{av} depends on two independent parameters, ϵ and τ_0 (or, equivalently, the map strength S). The parameter ϵ is related to the characteristic nonlinear length, $L_{nl} = 1/(\gamma P_{av})$, where P_{av} is the average pulse power, by

$$\epsilon = L_{\rm map}/(L_{nl}I_0). \tag{21}$$

As we have mentioned earlier, stationary propagation of a DM soliton is supported by a balance between the nonlinearity and the average dispersion, the stronger local dispersion providing only the functional form of the pulse. This means that the characteristic length associated with nonlinearity and average dispersion should be much larger than the local dispersion length, in order to ensure stable pulse propagation. This results in the condition $L_{nl} \gg L_{\rm map}$, or $\epsilon \ll 1$. In our numerical simulations we observe that pulses remain stable when $L_{nl} \approx L_{\rm map}$, and sometimes even when $L_{nl} \approx L_{\rm map}/2$, with only a few percent of their energy being shed into radiation. However, already for $L_{nl} \approx L_{\rm map}/3$ we never found a stable DM soliton. Thus, in most cases, the condition

$$L_{\rm map} < L_{nl} \tag{22}$$

plays the role of an additional upper bound on D_{av}. Using relations (21), (10), and (6), this can be rewritten as

$$D_{av} < \frac{(\mathrm{Re}I_2/\sqrt{2} + \epsilon C_R/8)\tau_0^2 T_{\rm DM}^2}{I_0 L_{\rm map}} \left(\frac{2\pi c}{\lambda^2}\right) \tag{23}$$

which is solved iteratively using (6). Since this upper bound on D_{av} is not as rigorously set as the one imposed by the GH jitter and pulse interaction, we use it as a guidance only. That is, we always verify whether the DM soliton is stable when (23) is not satisfied.

III. Optimization Procedure and Fiber Parameters

One map configuration that we consider has $L_{\rm map} = L_{\rm amp}$. There, we have two adjustable parameters. One is the location of the amplifier inside the compensating section of fiber. The other is the ratio $T_{\rm FWHM}/T_B$, which we vary between 0.12 and 0.28 with an increment 0.01. We observe that the GH jitter and the SNR yield the optimal ΔD_{av} when the amplifier is located at either end of the compensating section of fiber, whereas pulse interaction is the least restrictive when the amplifier is close to the middle of that section. However, due to the strong dependence of the map strength (12) on the pulse width, the latter is found to affect the system performance significantly more than the amplifier location does.

Another map configuration has $L_1 = NL_{\rm amp}$, where N is an integer. There, each of the first N amplifiers exactly compensates the loss in the preceding segment of length L_1/N of the fiber with dispersion D_1, and the $(N+1)$st amplifier compensates the loss in the shorther fiber section. The location of the amplifiers in this case is fixed, and the only adjustable parameter is the pulse width. For the third map configuration, with $L_{\rm amp} = NL_{\rm map}$, we fix the amplifier location to be at the beginning of every Nth map period. There, as well as for the map with distributed amplification, the pulse width is also the only adjustable parameter.

We use (16) to determine the lower bound for D_{av}, and the more restrictive of expressions (20) and (23) to determine the upper bound. For fixed values of the bit rate, propagation distance, and BER, our main result is the dependence of the optimal range of D_{av} on the map period $L_{\rm map}$, where optimization is done with respect to the adjustable parameter(s). By the optimal, we mean such a range ΔD_{av}, for which the quantity $\Delta D_{av} T_{\rm FWHM}$, proportional to the allowed number of WDM channels, $N_{\rm channels}$, is the maximum. Indeed, if we assume that

$$D_{av} \le \frac{3\sqrt{2\pi}(1/B)^2\tau_0 T_{\rm DM}^3(2\pi c/\lambda^2)}{z^3(2Q_{\rm GH})^2\gamma L_{\rm map}^2\left(\mathrm{Re}I_2 + \epsilon C_R/(4\sqrt{2})\right) n_{sp}h\nu(G-1)(L_{\rm map}/L_{\rm amp})} \tag{19}$$

TABLE I
FIBER PARAMETERS

Type of fiber	Dispersion [ps/nm/km]	Dispersion slope [ps/nm^2/km]	Power loss [dB/km]	$\gamma = 2\pi n_2/(\lambda A_{\text{eff}})$ [a] [(W km)$^{-1}$]
SSMF	17	0.056	0.2	1.3
DSF	-1.5	0.07	0.25	1.9
DCF[b]	-104	-0.35	0.5	5.2

the wavelength separation $\Delta\lambda$ between channels is a fixed multiple of the single-channel spectral width, then $\Delta\lambda \propto T_{\text{FWHM}}$. The maximum allowed number of channels is

$$N_{\text{channels}} = \Delta D_{av}/(|\partial D_{av}/\partial\lambda|\Delta\lambda) \tag{24}$$

where $\partial D_{av}/\partial\lambda$ is the average dispersion slope. Two obvious ways to increase N_{channels} are to either increase ΔD_{av} (or $\Delta D_{av}/\Delta\lambda$) or decrease $|\partial D_{av}/\partial\lambda|$ by carefully designing the compensating fiber. In this study we focus on maximizing the former parameter. Now, dispersion management is most effective when the average dispersion is much less than the local dispersion in the map. Consequently, we expect that to achieve large ΔD_{av}, we need the map to be composed of fiber sections with high dispersion coefficients. (Note that using high-dispersion fiber is also beneficial for suppression of WDM-induced impairments.) Table I lists relevant parameters of the existing types of fiber, that we consider in this study. The acronyms in the left-most column stand for the standard single-mode (SSMF), dispersion-shifted (DSF), and dispersion-compensating (DCF) fibers.

As we said in Section II-B, we do not have an analytic formula for the effect of pulse interaction and thus have to evaluate it numerically for the maximum value of D_{av} allowed by the CH jitter. Whenever we find $\delta\tau_{int}/T_B > 0.4$, we declare that the interaction prohibits the transmission. Since the interaction strength is proportional to the average dispersion [23], transmission would still be possible for some lower value of D_{av}. However, without an analytic expression for the effect of pulse interaction, we are unable to efficiently determine the corresponding upper bound.

IV. RESULTS

A. Transpacific Distance

Here we consider propagation over 10 000 km and require that the BER at the output be at most 10^{-12}. We consider the bit rate of 10 Gb/s per channel and the map configuration with $L_{\text{map}} = L_{\text{amp}}$.

The GH jitter suppression is most efficient in strong maps, since then the EEF, which mainly determines the suppression factor in comparison with the uniform-dispersion case, is large. On the other hand, pulse interaction rapidly increases as the map strength S exceeds a certain value, which in the lossless case was found to be about 1.6 [24]. Moreover, the condition (23) is violated for too large values of the EEF (recall that EEF $\sim 1/\text{Re}I_2$). Thus, one needs to use a map with S in the range between 1–2. (Let us note that the theory of DM soliton interaction, found in [8], [23], is applicable for larger values of the map strength ($S > 2$) than we consider here.) As follows from (12) and Table I, the only combination of fibers for which this range of S is possible, when the soliton width is about 1/5th of the bit slot and L_{map} is about 30–40 km, is the SSMF + DCF. The corresponding range of allowed values of D_{av} is plotted in Fig. 1(a). The reasons limiting this range can be understood from the behavior of the optimal pulse width parameter, T_{FWHM}/T_B, the associated optimal map strength, S, and the pulse interaction parameter, $\delta\tau_{int}/T_B$ [Fig. 1(b)]. For all values of L_{map} considered here, the optimal map strength is noticeably larger than 1.6, around which we expect pulse interactions to be the weakest. This rather large S appears to be necessary to suppress the GH jitter, which increases with $L_{\text{map}} = L_{\text{amp}}$ due to the exponential increase of the amplifier gain, $G = \exp(\alpha L_{\text{amp}})$; cf. (17). On the other hand, the increase of the parameter T_{FWHM}/T_B, seen in Fig. 1(b), clearly indicates that, to limit pulse interaction, S has to be reduced. However, this increase of the pulse width can limit the interaction via the reduction of S only up to a certain point, because for too large a width, the pulses begin

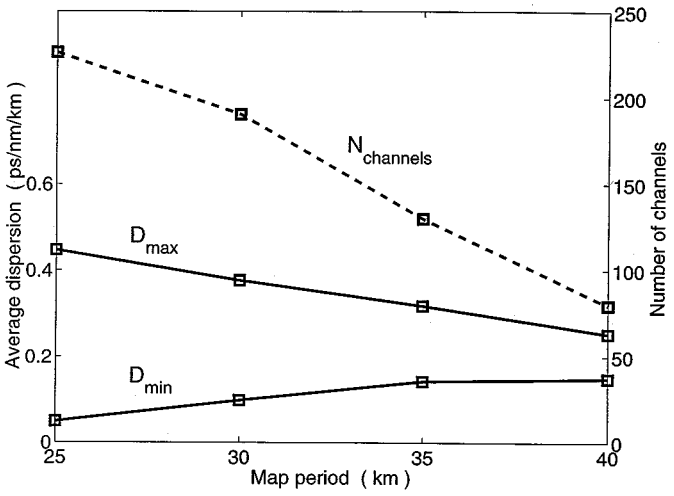

(a)

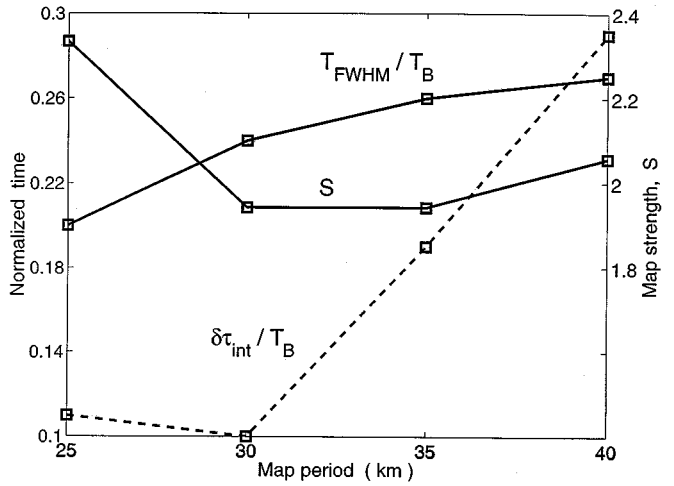

(b)

Fig. 1. SSMF + DCF, $Z = 10\,000$ km, $B = 10$ Gb/s/channel, $L_{\text{map}} = L_{\text{amp}}$. (a) Range of D_{av} (solid) and N_{channels} (dashed); (b) Ratios of the optimal pulse width (solid, left axis) and the decrease in pulse separation (dashed, left axis) to the bit slot, and the optimal map strength (right axis).

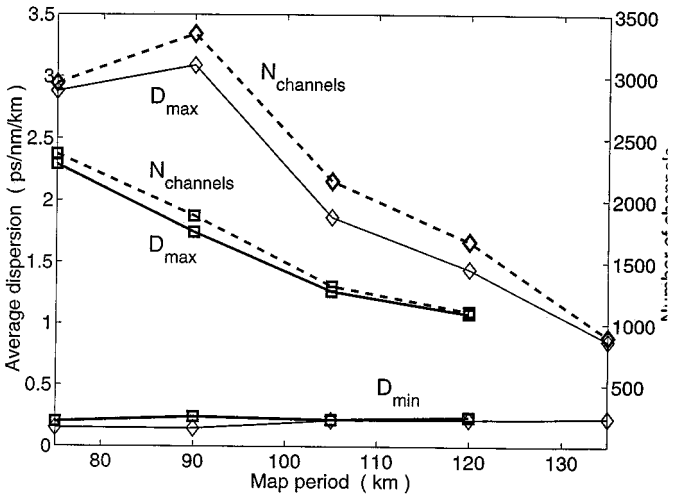

Fig. 2. Same as in Fig. 1(a), but $B = 5$ Gb/s/channel. Squares (diamonds): configuration with $L_1 = 2L_{\rm map} (L_1 = 3L_{\rm map})$.

to overlap too much, causing the interaction to increase. The increase of the interaction parameter is clear from Fig. 1(b). In fact, the interactions render the system unusable soon after $L_{\rm map} = L_{\rm amp}$ exceeds 40 km.

The dashed line in Fig. 1(a) shows an estimate for the maximum number of channels, calculated using (24) and $\Delta\lambda = 0.8$ nm for the interchannel separation. This $\Delta\lambda$ corresponds to roughly five spectral widths of a single channel. For a rather small range of D_{av}, e.g., $\Delta D_{av} \approx 0.2$ ps/nm/km at $L_{\rm map} = 35$ km, the number of channels is still very large ($N_{\rm channels} \approx 120$) due to the very small average dispersion slope of the configuration SSMF + DCF. It is, therefore, quite likely that the limits for the total transmission capacity in this case are set not by the GH jitter and pulse interactions, but rather by the WDM impairments and the availability of amplifiers with a flat gain over the bandwidth of 96 nm ($= 120 \times 0.8$ nm) and a high output power. The same remark also pertains to the results shown in Fig. 2 below.

We performed similar calculations for the same combination SSMF + DCF, with distributed amplification, which we assumed to exactly compensate for the fiber loss. For map periods of 25 and 30 km, the average dispersion range is about 40% larger than in the system with lumped amplification. This is due to the larger upper bound for D_{av} allowed by the GH jitter (because the amplifier noise is reduced by a factor $(G-1)/(\alpha_{av}L_{\rm map})$. However, already for $L_{\rm map} = 35$ km, that upper bound becomes so high that pulse interaction prohibits the transmission.

From this example, we make the following observations as to how the performance of the SSMF + DCF configuration could be further improved. 1) If, instead of the SSMF with $D = 17$ ps/nm/km, one could use a fiber with a lower value of dispersion, one would effectively decrease S, and thus would be able to use pulses with smaller widths. Then pulse interaction would limit the transmission less severely. 2) One could use the idea of "dense" DM, proposed in [26], where the map period is an integer fraction of the amplification distance: $L_{\rm map} = L_{\rm amp}/N$. With small enough $L_{\rm map}$, narrower pulses (for the same bit rate) could be used. This gives one the freedom to operate at values of the map strength that are high enough to yield significant jitter suppression. At the same time, even though pulse spreading is larger in those stronger maps, pulse interaction can still be not too strong owing to an increased pulse separation relative to the pulse width. We defer detailed examination of this venue of performance improvement until the next section.

In the remainder of this section, we examine another way of increasing the total transmission capacity, which is evident from (19) and (23). 3) For a fixed map strength, the upper bound for D_{av} set by the GH jitter is inversely proportional to the *cube* of the bit rate (since $\tau_0 T_{\rm DM} \sim T_{\rm FWHM} \sim 1/B$). If the allowed range ΔD_{av} were set by the GH jitter alone, the total transmission capacity ($= N_{\rm channels} \times$ (single-channel bit rate)) would increase by eight times if one uses 5-Gb/s channels instead of 10-Gb/s ones. Similarly, the other upper bound given by (23) would yield a four-time increase in that case. The lower bound would also decrease by a factor of two [cf.(16)], but this would not affect ΔD_{av} as much as the increase of the two upper bounds [cf. Fig. 1(a)]. Thus, the total capacity can, at least in principle, increase by four to eight times, if one decreases the bit rate per channel by a factor of two.

To verify this, we modified our map so as to keep the map strength approximately the same as. in the case of $B = 10$ Gb/s/channel, which meant we had to use the map period about three to four times larger than that in the latter case. The most appropriate configuration is then the one with $L_1 = NL_{\rm amp}$, where L_1 is the length of the first fiber section in the map. We performed calculations for the cases when $N = 2$ and $N = 3$, and set $\Delta\lambda = 0.4$ nm. The results for ΔD_{av} and $N_{\rm channels}$ are presented in Fig. 2, from which we see that using 5-Gb channels increases the total capacity by a factor of about five compared with the case of 10-Gb channels.

B. Transatlantic Distance

For the single-channel bit rate of 20 Gb/s, one cannot use a dispersion map composed of the combination of the SSMF + DCF fibers and having $L_{\rm map} \geq L_{\rm amp}$, simply because the corresponding map strength is too high (>7) for all realistic values of the amplifier spacings. To reduce the map strength, one option is to use the combinations DSF + SSMF, in which the longer section of fiber has significantly lower dispersion than the SSMF. However, even in that case, it is difficult to find values of adjustable parameters in our optimization scheme which would yield a positive range ΔD_{av}. This occurs because the upper bound for D_{av}, set by the GH jitter, is proportional to $(1/B)^3$ and thus is dramatically decreased for 20 Gb/s compared with the case of 10 Gb/s. In order to increase that upper bound to a level where it would again make sense to consider optimization of the system, we need to reduce the propagation distance by about the same factor by which we increased the bit rate [cf. (19)]. In this ection, we consider $Z = 6000$ km, which is a typical transatlantic distance. In addition, we set the allowed BER to a lower value of 10^{-6}, assuming that forward error correction can bring it down to an acceptable level. Expectedly, we then find that ΔD_{av} for the DSF+SSMF combination is as large as that for the map considered in Section IV-A [compare Fig. 1(a) with the first line in Table II]. Note, however, that the number of WDM channels for the DSF + SSMF combina-

TABLE II
AVERAGE DISPERSION RANGE FOR VARIOUS MAPS

Distance km	Bit rate Gb/s/channel	Fiber combination	L_{map} km	L_{amp} km	D_{min} ps/nm/km	D_{max} ps/nm/km	Optimal T_{FWHM}/T_B
6,000	20	DSF+SSMF	30–55	$= L_{\text{map}}$	0.02–0.03	0.31–0.24	0.18–0.21
6,000	20	SSMF+DCF	5	30–55	0.02	0.43–0.29	≈ 0.2
6,000	10	SSMF+DCF	10–12	30–55[a]	0.02–0.04	2.88–1.78	≈ 0.15
3,000	40	DSF+SSMF	10–16	80 or 84 [a]	0.02	0.10–0.09	0.19–0.24
3,000	20	DSF+SSMF	40	80	0.05	0.40	0.21

tion must be very small (about 2), due mostly to the much larger average dispersion slope of this fiber combination.

One might be tempted to consider the same trick as that used in Section IV-A, i.e., to use $B = 10$ Gb/s instead of 20 Gb/s per channel, to boost the total transmission capacity of the system. However, this does not work for the DSF+SSMF combination, simply because D_{av} cannot be increased much without violating the condition $D_{av} \ll D_{\text{local}}$. To get around this problem, one needs to use the combination SSMF + DCF, where the local dispersion is much higher. In order to keep the map strength not too high, one has to choose the map period to be smaller than the amplification spacing. Thus we are naturally led to considering the "dense DM" [26] configuration with $L_{\text{map}} = L_{\text{amp}}/N$, where, for $B = 10$ Gb/s/channel, L_{map} should be about 10 km in order to have the map strength not too high.

The maximum allowed ranges of D_{av} for the combination SSMF + DCF and for the bit rates 20 and 10 Gb/s, are reported in Table II (lines 2 and 3). For $B = 20$ Gb/s, we set $L_{\text{map}} = 5$ km and vary N accordingly. For $B = 10$ Gb/s, we set $N = 3$ for $L_{\text{amp}} = 30$ and 35 km, $N = 4$ for $L_{\text{amp}} = 40$ and 45 km, and $N = 5$ for $L_{\text{amp}} = 50$ and 55 km, so that L_{map} is always between 10–12 km. For the 20 Gb/s case, the optimum pulse width is set mostly by a compromise between the GH jitter and pulse interaction, with T_{FWHM} being close to 20% of the bit slot. As in Section IV-A, we note a significant increase of the total transmission capacity when using the single-channel bit rate 10 Gb/s instead of 20 Gb/s. For the 10-Gb/s case, we find that the low-power condition (22) severely decreases the upper bound for D_{av} that is otherwise allowed by the GH jitter. The optimum value of T_{FWHM}/T_B is found to be between 0.15–0.16 for all values of L_{amp}; for smaller pulse widths (which imply smaller L_{nl}), the DM solitons are not stable. Thus, if smaller values of L_{map} were used in this case, the allowed range ΔD_{av} would have been larger.

C. Terrestrial Distance

If we want to increase the single-channel bit rate to 40 Gb/s, we need to consider shorter propagation distances, as explained in the preceding section. As a challenging terrestrial scale, we take $Z = 3000$ km, and the amplifier spacing is the standard 80 km. To have values of the map strength in the range between 1–2, we are required to consider dense DM configuration even for the combination DSF + SSMF. For this combination, we can take L_{map} to be anywhere between 10–16 km to transmit two or three 40-Gb channels spaced 1.6 nm apart (cf. Table II). Similarly to the results of the preceding subsections, using 20-Gb instead of 40-Gb channels significantly increases the total transmission capacity. Note that the condition $D_{av} \ll D_{\text{local}}$ is *not* violated in this case.

Finally, we report on an interesting observation, which we made when trying to increase the transmission capacity by using the combination SSMF + DCF for the dispersion map. Transmission of 40-Gb channels in such a map would require extremely short map periods of less than 1.5 km. For this reason, we concentrate on 20-Gb channels. Recall that we have already demonstrated viability of 20-Gb/s transmission in SSMF + DCF maps in the previous section. Surprisingly, now, for twice as short a distance, we could not find a range of parameters where transmission would be possible near or at the upper bound for D_{av} set by the GH jitter. The reason behind this is the following. The amplifier spacing of 80 km, used for terrestrial systems, is about twice of that considered in Section IV-B. The pulse power at the amplifier, that is needed to guarantee a given average power, increases exponentially with L_{amp} and leads to a corresponding increase in pulse interaction, which appears to be the main limiting factor in this case. We expect that the use of distributed amplification would lead to a decrease of the pulse peak power and thus make transmission possible. In fact, we expect that, it would provide a greater range of D_{av} than we found in Section IV-B for the same map configuration.

V. CONCLUSION

This study addresses optimization of parameters of long-haul DM soliton systems while considering the impairments set only by the amplifier noise and pulse interaction. From the results presented in Section IV we draw the following four main conclusions.

First, in order to have the upper bound for D_{av} sufficiently large, the smaller of the dispersion coefficients of the two fiber sections has to be much larger than D_{av}, so as to ensure the condition $D_{av} \ll D_{\text{local}}$. If the latter condition is not satisfied, the dispersion map cannot be expected to significantly improve the system performance over that in the uniform-dispersion case. Thus, the SSMF + DCF combination is expected to provide a lager ΔD_{av} than a combination involving some type of a DSF. In addition, WDM impairments are suppressed by high local dispersion.

Second, in order to avoid large pulse spreading (which leads to increased pulse interaction) when operating at more than 10 Gb/s in a SSMF, one needs to use "dense DM" configuration where the map period is chosen to be a fraction of the amplification spacing. This allows one the freedom of using sufficiently

narrow pulses. The latter leads to more efficient jitter suppression via the increased EEF, and at the same time, pulse interaction is reduced because of an increased pulse separation relative to their width. Let us note, however, that using dense DM does not always help to reduce pulse interaction. Even though the condition $L_{n1} \gg L_{\rm map}$ may be satisfied for very short maps, the nonlinear length can still be hundreds of times shorter than the transmission distance. Then pulse interaction, whose effect is accumulated over that many nonlinear lengths, may become strong enough to prohibit the transmission. Thus a compromise value for $L_{\rm map}$, based on the above considerations, should be chosen.

Third, using distributed amplification can increase the allowed range ΔD_{av}, because the GH jitter in a distributedly-amplified system is reduced by a factor of $(\exp(\alpha L_{\rm amp})-1)/(\alpha L_{\rm amp})$ compared with that in a system with amplification spacing $L_{\rm amp}$. However, this increase of ΔD_{av} is less than the maximum possible increase, given by the above exponential factor, because the upper bound for D_{av} may be set by pulse interaction rather than by the GH jitter alone. On the other hand, as we noted in Section IV-C, maximum pulse power in a distributedly amplified system is less than that in a system with lumped amplification, which may help to reduce pulse interaction.

Fourth, using a lower bit rate per channel can significantly increase the total transmission capacity. This occurs because the maximum allowed range of D_{av} increases dramatically with the decrease of the bit rate. Moreover, WDM impairments are also ameliorated in systems using lower bit rates per channel. Specifically, tolerance to the timing jitter induced by collisions of DM solitons in different channels is inversely proportional to the bit rate [27]. For the nonreturn-to-zero (NRZ) transmission format, the impairments due to four-wave mixing and interchannel Raman cross-talk were shown to also be less severe for a WDM system based on a lower bit rate per channel [28]. Since these types of impairments are similar in character for the soliton and NRZ systems (compare, e.g., [13] and [28]), we believe that the conclusion stated in the beginning of this paragraph will hold true when all types of transmission impairments are taken into account. We note that this conclusion is not specific to DM systems; it certainly was made earlier in regards to both the soliton- and NRZ-based transmissions in uniform-dispersion systems. A new twist which is specific to DM systems is that the value of the bit rate per channel must be carefully chosen so as to ensure the main condition, $D_{av} \ll D_{\rm local}$ (cf. Section IV-B).

Finally, we note that the results presented in Section IV for the SSMF + DCF map and indicating the possibility of having a total transmission capacity of several terabit per second should be interpreted with caution. Consider, for example, Fig. 2. It is not realistic that transmission of thousands of 5-Gb/s channels spaced at 0.4 nm would ever be possible in a single-mode fiber, because of the limitations imposed by the requirements on the amplifier gain uniformity and output power. Instead, Fig. 2 shows that single-channel impairments do not impose significant restrictions on transmission in that particular case. Thus, further optimization of the dispersion maps should focus on minimizing the WDM impairments.

APPENDIX

Here we present the explicit form of the terms C_I and C_R in (10). They are calculated by extending the method of [16] through the second order in ϵ and taking into account only the zeroth- and second-order Hermite–Gaussian functions. The same results could also be obtained by extending the equations of the variational method for the DM soliton through the same order.

We only write the form of C_I and C_R that is valid for map configurations with $L_{\rm amp} = L_{\rm map}$, $L_1 = NL_{\rm amp}$, and the distributedly-amplified case. For the "dense DM" configuration, with $L_{\rm amp} = NL_{\rm map}$, these expressions can be easily generalized.

$$\begin{aligned} C_I = &\int_0^1 dz \left(\tilde{I}_0(z) + \tfrac{3}{2}\mathrm{Re}\tilde{I}_4(z)\right) \int_0^z dz' (\mathrm{Re}\tilde{I}_2(z') - I_2) \\ &+ \int_0^1 dz \left(\tfrac{3}{2}\mathrm{Im}\tilde{I}_4(z)\right) \int_0^z dz' \mathrm{Im}\tilde{I}_2(z') \\ &+ \left(\tfrac{5}{2} I_0 - \tfrac{3}{2}\mathrm{Re}I_4 - 7\int_0^1 dz \left(z\tilde{I}_0(z)\right)\right) \\ &\cdot \left(\tfrac{1}{2} I_2 - \int_0^1 dz \left(z\mathrm{Re}\tilde{I}_2(z)\right)\right) \\ &+ \tfrac{3}{2}\mathrm{Im}I_4 \int_0^1 dz \left(z\mathrm{Im}\tilde{I}_2(z)\right) \end{aligned} \tag{A1}$$

$$\begin{aligned} C_R = &\int_0^1 dz \left(\tfrac{3}{2}\mathrm{Im}\tilde{I}_4(z)\right) \int_0^z dz' (\mathrm{Re}\tilde{I}_2(z') - I_2) \\ &+ \int_0^1 dz \left(\tilde{I}_0(z) - \tfrac{3}{2}\mathrm{Re}\tilde{I}_4(z)\right) \int_0^z dz' \mathrm{Im}\tilde{I}_2(z') \\ &+ \left(-\tfrac{5}{2} I_0 - \tfrac{3}{2}\mathrm{Re}I_4 + 7\int_0^1 dz \left(z\tilde{I}_0(z)\right)\right) \\ &\cdot \int_0^1 dz \left(z\mathrm{Im}\tilde{I}_2(z)\right) \\ &- \tfrac{3}{2}\mathrm{Im}I_4 \left(\tfrac{1}{2} I_2 - \int_0^1 dz \left(z\mathrm{Re}\tilde{I}_2(z)\right)\right) \end{aligned} \tag{A2}$$

where functions $\tilde{I}_n$ are defined in (11). We note that for sufficiently high power of a DM soliton (equivalently, suffiently large ϵ) it is more accurate, and probably even easier, to find the initial value for the soliton chirp and the relation between D_0 and τ_0 by directly solving the variational equations, as in [18], [34], [35]. In this study, however, finding the $O(\epsilon)$ corrections to (10) using (A1) and (A2) was quite adequate.

REFERENCES

[1] F. M. Knox, W. Forysiak, and N. J. Doran, "10-Gbt/s soliton communication systems over standard fiber at 1.55 μm and the use of dispersion compensation," *J. Lightwave Technol.*, vol. 13, pp. 1955–1962, 1995.

[2] C. R. Menyuk, "Non-Gaussian corrections to the Gordon–Haus distribution resulting from the soliton interactions," *Opt. Lett.*, vol. 20, pp. 285–287, 1995.

[3] R.-M. Mu, V. S. Grigoryan, C. R. Menyuk, E. A. Golovchenko, and A. N. Pilipetskii, "Timing-jitter reduction in a dispersion-managed soliton system," *Opt. Lett.*, vol. 23, pp. 930–932, 1998.

[4] N. J. Smith, W. Forysiak, and N. J. Doran, "Reduced Gordon–Haus jitter due to enhanced-power solitons in strongly dispersion-managed systems," *Electron. Lett.*, vol. 32, pp. 2085–2086, 1996.

[5] M. K. Chin and X. Y. Tang, "Quasistable soliton transmission in dispersion-managed fiber links with lumped amplifiers," *IEEE Photon. Technol. Lett.*, vol. 9, pp. 538–540, 1997.
[6] T. I. Lakoba, J. Yang, D. J. Kaup, and B. A. Malomed, "Conditions for stationary pulse propagation in the strong dispersion management regime," *Opt. Commune.*, vol. 149, pp. 366–375, 1998.
[7] R.-M. Mu, V. S. Grigoryan, E. A. Golovchenko, A. N. Pilipetskii, and C. R. Menyuk, "Optimizing the arrangement of optical amplifiers in a dispersion-managed soliton system," in *Proc. Opt. Fiber Commun. (OFC'98)*, San Jose, CA, Feb. 22–27, 1998, paper ThC5.
[8] M. Matsumoto, "Analysis of interaction between stretched pulses propagating in dispersion-managed fibers," *IEEE Photon. Technol. Lett.*, vol. 10, pp. 373–375, 1998.
[9] A. M. Niculae, W. Forysiak, and N. J. Doran, "Optimal amplifier location in strong dispersion managed soliton systems," in *Proc. Conf. Lasers and Electrooptics (CLEO'99)*, Baltimore, MD, May 23–28, 1999, paper CWC6.
[10] A. F. Evans and J. V. Wright, "Constraints on the design of single-channel, high-capacity (>10 Gb/s) soliton systems," *IEEE Photon. Technol. Lett.*, vol. 7, pp. 117–119, 1995.
[11] L. F. Mollenauer, "Method of nulling nonrandom timing jitter in soliton transmission," *Opt. Lett.*, vol. 21, pp. 384–386, 1996.
[12] L. F. Mollenauer and J. P. Gordon, "Birefringence-mediated timing jitter in soliton transmission," *Opt. Lett.*, vol. 19, pp. 375–377, 1994.
[13] T. I. Lakoba and D. J. Kaup, "Influence of Raman effect on dispersion-managed solitons and their interchannel collisions," *Opt. Lett.*, vol. 24, pp. 808–810, 1999.
[14] T. I. Lakoba and G. P. Agrawal, "Effects of third-order dispersion on dispersion-managed solitons," *J. Opt. Soc. Am. B*, vol. 16, Sept. 1999.
[15] T. I. Lakoba and D. J. Kaup, "Shape of stationary pulse in the strong dispersion management regime," *Electron. Lett.*, vol. 34, pp. 1124–1126, 1998.
[16] ——, "Hermite–Gaussian expansion for pulse propagation in strongly dispersion-managed fibers," *Phys. Rev. E*, vol. 58, pp. 6728–6741, 1998.
[17] S. K. Turitsyn, A. B. Aceves, C. K. R. T. Jones, and V. Zharnitsky, "Average dynamics of the optical soliton in communication lines with dispersion management: Analytical results," *Phys. Rev. E.*, vol. 58, pp. R48–R51, 1998.
[18] A. Berntson, N. J. Doran, W. Forysiak, and J. H. B. Nijhof, "Power dependence of dispersionmanaged solitons for anomalous, zero, and normal path-average dispersion," *Opt. Lett.*, vol. 23, pp. 900–902, 1998.
[19] N. A. Olsson, "Lightwave systems with optical amplifiers," *J. Lightwave Technol.*, vol. 7, pp. 1071–1082, 1989.
[20] J. W. Goodman, *Statistical Optics*. New York, NY: Wiley-Interscience, 1985, sec. 6.1, pp. 238–256.
[21] D. Marcuse, "Derivation of analytical expressions for the bit-error probability in lightwave systems with optical amplifiers," *J. Lightwave Technol.*, vol. 8, pp. 1816–1823, 1990.
[22] T. Okamawari, A. Maruta, and Y. Kodama, "Reduction of Gordon–Haus jitter in a dispersion-compensated optical transmission system: Analysis," *Opt. Commun.*, vol. 149, pp. 261–266, 1998.
[23] S. Kumar, M. Wald, F. Lederer, and A. Hasegawa, "Soliton interaction in strongly dispersionmanaged optical fibers," *Opt. Lett.*, vol. 23, pp. 1019–1021, 1998.
[24] T. Yu, E. A. Golovchenko, A. N. Pilipetskii, and C. R. Menyuk, "Dispersion-managed soliton interactions in optical fibers," *Opt. Lett.*, vol. 22, pp. 793–795, 1997.
[25] L. F. Mollenauer, P. V. Mamyshev, and J. P. Gordon, "Effect of guiding filters on the behavior of dispersion-managed solitons," *Opt. Lett.*, vol. 24, pp. 220–222, 1999.
[26] A. H. Liang, H. Toda, and A. Hasegawa, "High-speed soliton transmission in dense periodic fibers," *Opt. Lett.*, vol. 24, pp. 799–801, 1999.
[27] P. V. Mamyshev and L. F. Mollenauer, "Soliton collisions in wavelength-division-multiplexed dispersion-managed systems," *Opt. Lett.*, vol. 27, pp. 448–450, 1999.
[28] F. Forghieri, R. W. Tkach, and A. R. Chraplyvy, "Fiber nonlinearities and their impact on transmission systems," in *Optical Fiber Telecommunications IIIA*, I. P. Kaminow and T. L. Koch, Eds. San Diego, CA: Academic, 1997, ch. 8, pp. 248–251.
[29] T. Georges, "Bit-error rate degradation of interacting solitons owing to non-Gaussian statistics," *Electron. Lett.*, vol. 31, pp. 1174–1175, 1995.
[30] A. N. Pinto, G. P. Agrawal, and J. F. da Rocha, "Effect of soliton interaction on timing jitter in communication systems," *J. Lightwave Technol.*, vol. 16, pp. 515–519, 1998.
[31] V. S. Grigoryan, C. R. Menyuk, and R.-M. Mu, "Calculation of timing and amplitude jitter in dispersion-managed optical fiber communications using linearization," *J. Lightwave Technol.*, vol. 17, pp. 1347–1356, 1999.
[32] A. N. Pilipetskii and C. R. Menyuk, "Suppression of the acoustic effect in soliton information transmission by line coding," *Opt. Lett.*, vol. 22, pp. 28–30, 1997.
[33] S. K. Turitsyn and V. K. Mezentsev, "Dynamics of self-similar dispersion-managed soliton presented in the basis of chirped Gauss–Hermite functions," *JETP Lett.*, vol. 67, pp. 640–646, 1998.
[34] Y. Kodama, "Nonlinear chirped RZ and NRZ pulses in optical transmission lines," Osaka Univ., Preprint.
[35] V. S. Grigoryan and C. R. Menyuk, "Dispersionmanaged solitons at normal average dispersion," *Opt. Lett.*, vol. 23, pp. 609–611, 1998.

T. I. Lakoba, photograph and biography not available at the time of publication.

G. P. Agrawal (F'96), photograph and biography not available at the time of publication.